Continuous Thermal Collapse of the Intrinsically Disordered Protein Tau Is Driven by Its Entropic Flexible Domain

ARTICLE *in* LANGMUIR · AUGUST 2012

Impact Factor: 4.46 · DOI: 10.1021/la302628y · Source: PubMed

Langmuir

Article

pubs.acs.org/Langmuir

Continuous Thermal Collapse of the Intrinsically Disordered Protein Tau Is Driven by Its Entropic Flexible Domain

Gabriele Ciasca,*[,†] Gaetano Campi,[‡] Anna Battisti,[§] Giuseppina Rea,[‡] Marina Rodio,[†] Massimiliano Papi,[∥] Petra Pernot,[⊥] Alexander Tenenbaum,[†] and Antonio Bianconi[†]

[†]Physics Department, Sapienza University, 00185 Rome, Italy

[‡]Institute of Crystallography, CNR, 00016 Monterotondo, Italy

[§]LISC, CMM-FBK and University of Trento, 38123 Povo, Italy

[∥]Institute of Physics, Catholic University, 00168 Rome, Italy

[⊥]Structural Biology Group, ESRF, 38043 Grenoble, France

Supporting Information

ABSTRACT: The tau protein belongs to the category of Intrinsically Disordered Proteins (IDP), which in their native state lack a folded structure and fluctuate between many conformations. In its physiological state, tau helps nucleating and stabilizing the microtubules' (MTs) surfaces in the axons of the neurons. Tau is mainly composed by two domains: (i) the binding domain that tightly bounds the MT surfaces and (ii) the projection domain that exerts a long-range entropic repulsive force and thus provides the proper spacing between adjacent MTs. Tau is also involved in the genesis and in the development of the Alzheimer disease when it detaches from MT surfaces and aggregates in paired helical filaments. Unfortunately, the molecular mechanisms behind these phenomena are still unclear. Temperature variation, rarely considered in biological studies, is here used to provide structural information on tau correlated to its role as an entropic spacer between adjacent MTs surfaces. In this paper, by means of small-angle X-ray scattering and molecular dynamics simulation, we demonstrate that tau undergoes a counterintuitive collapse phenomenon with increasing temperature. A detailed analysis of our results, performed by the Ensemble Optimization Method, shows that the thermal collapse is coupled to the occurrence of a transient long-range contact between a region encompassing the end of the proline-rich domain P2 and the first part of the repeats domain, and the region of the N-terminal domain entailing residues 80−150. Interestingly these two regions involved in the tau temperature collapse belong to the flexible projection domain that acts as an entropic bristle and regulates the MTs' architecture. Our results show that temperature is an important parameter that influences the dynamics of the tau projection domain, and hence its entropic behavior.

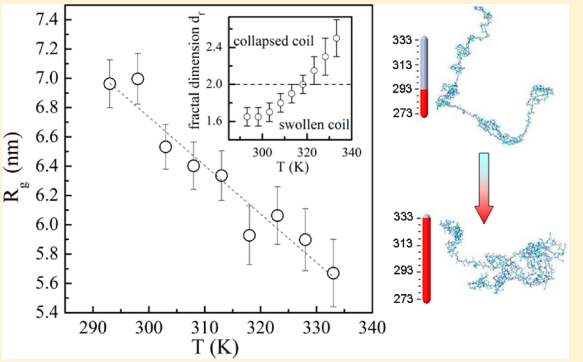

INTRODUCTION

It is well-known that structured proteins are generally denatured by heat. On the other hand, many intrinsically disordered proteins (IDPs) are known to be functionally resilient to temperature increase;[1] but their overall structure could depend on temperature. As a matter of fact, recent results have shown that high temperatures may induce a structural collapse in disordered protein.[2−4] This counterintuitive thermal collapse can occur both in IDPs and in unfolded proteins, resulting in a reduction of the radius of gyration R_g ranging from 5% to 35% of its initial value.[2,5−7]

IDPs lack a folded structure, displaying (in the most disordered cases) a random-coil-like average conformation when studied as an isolated polypeptide chain under physiological conditions.[8]

One of the largest totally disordered IDPs is the tau protein, which is a microtubule-associated protein expressed primarily in neurons; tau is found in the human central nervous system (CNS) in six isoforms, ranging from 352 to 441 amino acids.[9] In its physiological state, it promotes the growth and the assembly of microtubules.[10,11] Thanks to its high degree of conformational entropy, tau remains disordered even in the bound state *in vivo*, and functions as an entropic spacer/bristle that provides proper spacing between microtubules in the cytoskeleton.[1] Under pathological conditions, the same tau aggregates in paired helical filaments (PHFs), forming fibrils which in their turn form insoluble tangles. This phenomenon prevents tau from carrying out its physiological stabilization role, and, together with several other factors, is associated with

Received: June 29, 2012
Revised: August 7, 2012

   dx.doi.org/10.1021/la302628y | *Langmuir* XXXX, XXX, XXX−XXX

the degeneration of microtubules and the death of neurons.[12−15]

Because of its intrinsically disordered character, tau in solution explores a large region of the conformational space, fluctuating between a large number of conformers. Therefore, the application to the monomeric tau protein of standard structural techniques, such as macromolecular crystallography or electron microscopy, is not possible. In this framework, small-angle X-ray scattering (SAXS), which is a key technique in the study of a large class of biological systems,[16−20] provides a unique tool to obtain structural information on molecules belonging to the IDP category, in particular on tau in solution.[21−23]

In this work, we investigate the behavior of the longest CNS tau isoform, htau40 (441 residues), performing SAXS measurements at different temperatures in the range 293−333 K. Our measurements point out that the tau protein undergoes a relevant thermal collapse, with a reduction in the average radius of gyration of 18 ± 1% of its initial value. The occurrence of this phenomenon is shown by the behavior of the Kratky plot and of the fractal dimension d_f of the chain as a function of temperature. In order to get further insight into this phenomenon, we performed a conformational analysis by means of the Ensemble Optimization Method (EOM),[23] which showed that the probability of the molecule being in a conformation of high (low) R_g decreases (increases) when the temperature is increased. Our EOM analysis suggests that a high temperature favors the statistical occurrence of an interaction between the region entailing residues 80−150 and the region entailing residues 220−260 (i.e., between the end of the N-terminal domain and a region encompassing the end of the P2 domain and the first part of the repeats domain). A molecular dynamics (MD) simulation of the entire tau in explicit water solvent confirms the occurrence of such an interaction.

MATERIALS AND METHODS

Protein Preparation. The experiment has been performed using full length htau40 purchased from Sigma Aldrich, Milan, Italy (product code: T0-576). The protein powder was reconstituted and concentrated at nominal protein concentration of 2 mg/mL in 0.1× phosphate buffered saline (10× PBS: 1.3 M NaCl, 0.07 M Na_2HPO_4 and 0.03 M NaH_2PO_4, pH 7.4) by the QuickSpin protein concentration/buffer exchange (Dualsystem Biotech AG, Schlieren, Switzerland). Subsequently, the solution was centrifuged for 10 min at 10 000*g* and the supernatant filtered to eliminate aggregates. Protein quality was assayed by SDS-PAGE in 12% (w/v) polyacrylamide, according to Laemmli,[24] using a tau protein powder obtained from the same stock and subjected to the same thermal treatment used for the SAXS experiment. The gels were stained with Coomassie brilliant blue R-250. The SDS-PAGE analysis revealed the occurrence of a major protein band with the expected size (approximately 45 kDa), a 90% purity, and the absence of a significant amount of aggregates, both at 293 K and at higher temperatures. This analysis demonstrates that the thermal treatment used for the SAXS experiment does not induce protein aggregation.

SAXS Experiment and Data Analysis. SAXS measurements were acquired on the BioSAXS beamline (ID 14-3) at ESRF (Grenoble, France),[25] equipped with a 2D detector (Pilatus 1M, Dectris). The sample to detector distance for normal operation is 2.5 m, which allows a momentum transfer of $s = (4\pi \sin \theta/\lambda)$ in the range from 0.05 to 5.8 nm^{-1}. A volume of 50 μL of solution has been placed in a 1.8 mm diameter quartz capillary (mounted in vacuum) with a few tens of micrometer wall thickness, using an automated sample loader developed by EMBL in collaboration with ESRF.

The potential effect of radiation damage has been evaluated performing a 25 s exposure at constant temperature (293 K) without observing any radiation damage. In the experiment, we have used an exposure time of 3 s at each temperature to avoid a possible radiation damage. The sample was initially at room temperature (293 K), and the transfer of the sample to the measurement cell took place at the same temperature. Once the sample was transferred, the stepwise process of heating and SAXS data acquisition began. The BioSAXS beamline is equipped with a thermal control that allows the heating and the temperature monitoring of the sample cell. The measurements were performed in steps of 5 K, in the 293−333 K temperature range. After each heating step, we waited 10 min before acquiring the data, a time more than sufficient to let the capillary, the liquid, and the solute thermalize.

Solvent scattering was measured in the same capillary sample holder to allow for subtraction of the background scattering. Spectrophotometric determination of the actual concentration of tau in solution is not reliable.[21,22] As a consequence, the molecular mass of the protein cannot be obtained by standardization with a protein of known molecular mass.

An explicit description of the structural ensemble of the tau protein, which takes properly into account the coexistence of multiple conformations in solution, has been obtained by the EOM software package.[23,26] A pool of 10 000 representative backbone models of the protein has been created using the program RANCH. The theoretical scattering intensities corresponding to these models have been calculated by means of the program CRYSOL. These intensities have then been used by the genetic algorithm GAJOE to select from the initial pool an ensemble of conformers, the theoretical scattering curves of which provide, on the average, the best fit of the experimental SAXS data. The following GAJOE parameters were set: number of generations, 1000; number of ensembles, 50; number of curves per ensemble, 20; number of mutations per ensemble, 10; number of crossings per generation, 20. Two more original EOM pools, with a different numbers of original conformers, have been used to test the results obtained with the first pool.

Molecular Dynamics Simulation. A molecular dynamics computer simulation of tau has been performed at T = 333 K using the GROMACS software package[27] and an explicit water solvent at pH = 7.[28,29] Because of the intrinsically disordered nature of this protein and the consequent lack of a crystallographic 3D structure, the simulation started from an extended structure produced by an ad hoc procedure, which we have used in ref 28 to obtain the first MD simulation in explicit solvent of the entire tau at 300 K. This procedure starts from the primary sequence of the molecule to produce a multirod 3D structure, which is then dynamically evolved in vacuo so that it can flex until its gyration radius reaches the experimental value; at this point, the molecule is embedded in explicit water solvent, and allowed to relax for a short time at constant temperature and pressure. The final configuration of the molecule reached in this procedure is the starting point of a MD simulation at constant temperature (Berendsen thermostat) and constant pressure (Parrinello-Rahman pressure coupling). The initial configuration was obtained at T = 300 K, and was used also to start the simulation at T = 333 K, in order to better highlight the effect of the difference in temperature in the two cases. A contact map at 333 K computed over a time of 4 ns has been obtained and compared to a previously published contact map at 300 K.[29]

RESULTS

SAXS Results. Small-angle X-ray scattering measurements on the same tau sample in solution were performed in the temperature range 293−333 K, with a 5 K step. In Figure 1 (left panels), we report the scattering curves of tau in solution as a function of temperature. Only selected curves $I(s)$ have been reported, namely, at 293 K (panel a), 308 K (panel b), 318 K (panel c), and 333 K (panel d). Up to 318 K, one can distinguish three different regions in the scattered intensity $I(s)$

dx.doi.org/10.1021/la302628y | Langmuir XXXX, XXX, XXX−XXX

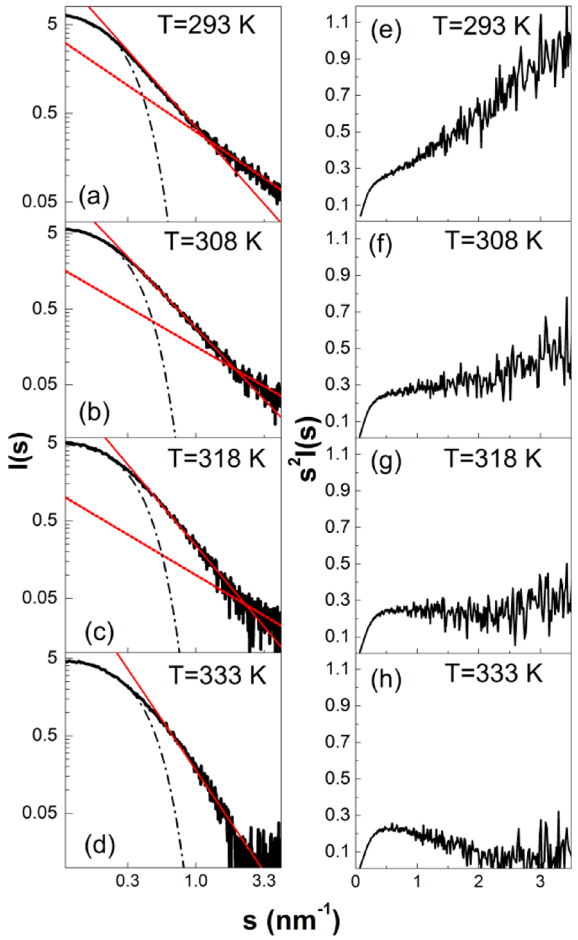

Figure 1. Left panels: (a–d) SAXS profiles of protein tau at different temperatures. The experimental data are displayed as a black continuous line. The fits, obtained assuming a Gaussian coil model, are displayed as black dash-dotted lines in the Guinier region (low s), continuous red lines in the power law region (intermediate s), and red dotted lines in the rodlike region (high s). Right panels: (e–h) Kratky plots showing the collapse of tau in solution as a function of temperature.

(Figure 1a–c): (i) a Guinier regime in the first part of the plot (black dash-dotted lines); (ii) a power law decay, $I(s) \sim s^{-d_f}$ at intermediate s, where d_f is the fractal dimension of the polimer in solution (red continuous line); (iii) a rodlike scattering $I(s) \sim s^{-1}$ at high values of s (red dotted lines). At temperatures higher than T = 318 K (Figure 1d), only two different regions are observed, the Guinier regime ($s < 0.2$ nm^{-1}) and the power law regime ($s > 0.2$ nm^{-1}), whereas the extended, rodlike region is not observed.

In the right panels of Figure 1, we show the thermal response of the Kratky plots ($s^2I(s)$ vs s). Dramatic changes in the $s^2I(s)$ shape can be observed with increasing temperature. The increase of $s^2I(s)$ at high s, observed in Figure 1e, suggests that the native protein is in an extended state at T = 293 K. Increasing the temperature, a continuous change occurs between the extended and a compacted state. A relevant compaction can be observed at 333 K (Figure 1h), as demonstrated by the arising of a peak in the Kratky plot.

To obtain further information on the compaction of tau, we have analyzed the scattering curves using the EOM. EOM first generates a pool of models spanning the protein's conformational space, and then selects from the pool by an iterative genetic algorithm the ensemble of conformers that best fits the experimental data at each temperature.[23,26] From these ensembles, we compute at each temperature the distribution of R_g values, which is reported in Figure 2. Under increasing

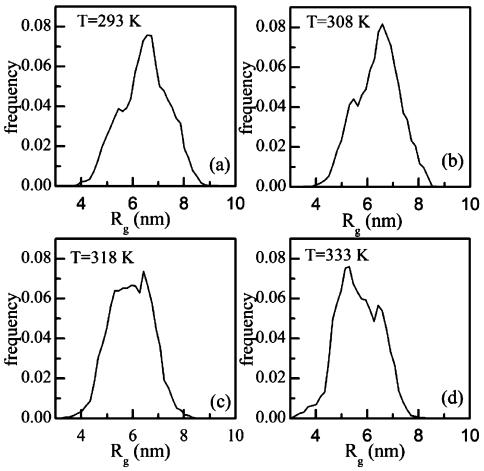

Figure 2. Distribution of the radius of gyration R_g of protein tau as a function of temperature.

temperature, a shift of the distribution peak toward lower values can be clearly observed. The intensity of the distribution around 6.7 nm decreases, whereas the intensity around 5.5 nm increases. This change in the relative probability of extended and compact conformers is reflected in the wings of the distributions: the probability of the most extended conformers diminishes as the probability of the most compact ones increases.

In Figure 3, we report the average R_g as a function of temperature, obtained by averaging the EOM over the selected

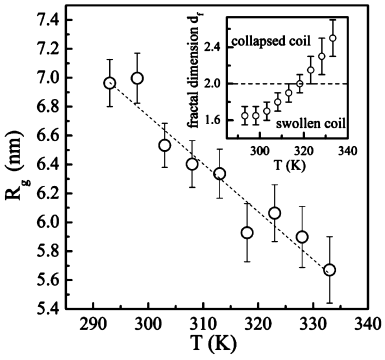

Figure 3. Average radius of gyration R_g versus temperature in the range 293–333 K. A linear fit of the points gives a slope of −0.29 ± 0.03 nm/K; fractal dimension d_f versus temperature (inset).

distribution of conformers. At 293 K, R_g assumes the value of 7.0 ± 0.2 nm, which is consistent within one standard deviation with the value obtained by a similar method,[21] and with the theoretical value expected for a 441 amino acid random coil in solution, which is 6.9 nm.[30] Increasing the temperature in the range 293–333 K, R_g decreases monotonously, within the experimental errors, from 7.0 ± 0.2 to 5.7 ± 0.3 nm. The total decrease amounts to 18 ± 1% of the initial R_g value. The compaction of tau is further confirmed by the behavior of d_f (inset of Figure 3), obtained by fitting the intermediate s region

dx.doi.org/10.1021/la302628y | Langmuir XXXX, XXX, XXX–XXX

of the scattering curves, which suggests a continuous transition between a swollen coil ($d_f < 2$) and a collapsed coil ($d_f > 2$).

In Figure 4, we report four contact maps of tau as a function of selected temperatures (293, 308, 318, and 333 K). These

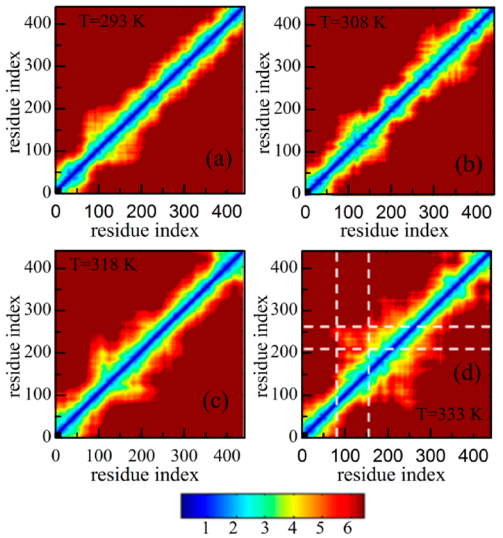

Figure 4. Average contact maps as a function of temperature. We highlight the arising of a long-range contact which occurs between the region entailing residues 220−260 and the region entailing residues 80−150. Different colors identify different distances (in nanometers).

maps have been computed by the average $C_\alpha - C_\alpha$ pair distances of all EOM selected conformers, weighted according to their frequency (Figure 2). The maps exhibit different patterns at different temperatures, showing a complicated temperature dependence; altogether, the compaction produced by the increase in temperature over the whole experimental range is clear when one compares T = 293K with T = 333K. At 333 K, an interaction between the region entailing residues 80−150 and the region entailing residues 220−260 (i.e., the end of the N-terminal domain and a region encompassing the end of the proline-rich P2 domain and the first part of the repeat domain) arises.

MD Simulation Results. Molecular dynamics simulation provides detailed information on the protein structure at the atomic level. Therefore, we decided to use MD simulation to test the occurrence of the wide ranging contact shown in Figure 4d. To verify this finding, a MD computer simulation of tau has been performed at T = 333 K using the GROMACS software package and an explicit water solvent at pH = 7,[27,28] and compared to a previous simulation done at T = 300 K for the same system and with the same method.[29] Both simulations started from a configuration produced in vacuo with the procedure described in ref 28; after an evolution of about 6 ns, the system reached a stationary state at both temperatures, corresponding respectively to an average R_g = 6.0 nm at T = 300 K and to an average R_g = 4.6 nm at T = 333 K; this temperature induced compaction amounts to a 23% reduction of the gyration radius, which is larger than, but of the order of, the experimental compaction. In Figure 5, we show two contact maps, computed at T = 300 K (panel a) and T = 333 K (panel b) over 4 ns, after the molecular structure has reached a stationary state at the corresponding temperature. The two contact maps are quite similar, with an exception made for the regions entailing residues 80−150 and residues 190−250. The

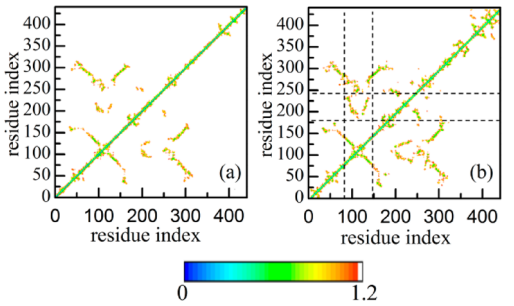

Figure 5. Contact maps computed by molecular dynamics simulation at T = 300 K (panel a, from ref 29) and T = 333 K (panel b). The arising of a long-range contact occurring at 333 K between the residues 190−250 and the region entailing residues 80−150 is highlighted by the dashed lines. Different colors identify different distances (in nanometers).

comparison of the two maps highlights the arising at 333 K of a wide ranging contact between these two regions, which was not present at 300 K, confirming the EOM analysis of the SAXS results (Figure 4d).

DISCUSSION

Our SAXS experiment shows that the tau protein undergoes a strong continuous thermal collapse under increasing temperature, which induces a reduction in R_g of 18 ± 1% when the temperature is increased in the range 293−333 K. This result is further confirmed by the behavior of the Kratky plot and of the fractal dimension d_f, which is a key parameter to investigate structural changes in several proteins.[31,32]

The occurrence of a thermal collapse has been demonstrated in several proteins, both natively disordered or unfolded by chemical denaturation. In particular, a collapse of 13 ± 3% and 15 ± 2% in R_g has been observed by fluorescence resonance energy transfer (FRET), respectively, for prothymosin, a highly hydrophilic intrinsically disordered protein, and for the small cold shock protein CspTm denaturated in guanidinium chloride (GdCl).[2] Moreover, the small acid-denaturated protein BBL exhibits a strong collapse (35% in R_g between 276 and 363 K), as demonstrated by FRET,[5] whereas ribonuclease T1 and ribonuclease A exhibit a slight collapse, of the order of 5%, of the initial hydrodynamic radius.[6]

Interestingly, the collapse of the hydrophilic tau is of similar extent (18% in R_g) as the collapse of the highly hydrophilic IDP prothymosin.

As in our case, all these collapses are continuous in temperature, which hints at a common mechanism underlying this phenomenon. Very recently, a compaction of tau of an extent similar to the one presented here has been reported by Shkumatov and co-workers.[4] They observed a reduction of R_g from 6.6 to 5.5 nm between 283 and 323 K, without acquiring intermediate temperatures. The measured extent of the compaction is in agreement with our measurements. Shkumatov and co-workers report that the temperature dependent compaction only takes place when a fast temperature jump is imposed on the sample (both upward and downward), whereas the protein remains identical at high and low temperature if it is kept at constant temperature. This aspect appears to be in contrast to our experimental results and deserves more exhaustive study.

The question of the interaction between distant segments of tau has been studied experimentally at room temperature by

dx.doi.org/10.1021/la302628y | Langmuir XXXX, XXX, XXX−XXX

Mukrasch and co-workers.[14] In particular, paramagnetic relaxation enhancement (PRE) of NMR signals has proved that monomeric tau in solution exhibits several transient contacts between residues which are far apart in the protein primary sequence. Among these, a transient long-range contact is established between the central domain entailing the residue 239 and residues 80−150 of the N-terminal domain. As suggested by our average contact maps (Figure 4, panel d), this interaction between the end of the P2 proline-rich domain and the region entailing residues 80−150 seems to become statistically relevant at 333 K, where the strongly collapsed state is observed. The occurrence of this interaction implies that, at least transiently, the projection domain (i.e., the most flexible domain of tau protein) folds, bringing the N-terminal region closer to the central part of the chain. The presence of a far reaching contact between domains far apart in the primary sequence agrees with the results of Shkumatov and co-workers, which show that the tau compaction is observed only in full length tau, not in the repeats domain alone.[4]

It could be noted that our average contact map at 293 K in Figure 4 does not show all the long-range contacts seen by Mukrasch and co-workers:[14] this means that they are lost in the average done in a SAXS experiment. On the other hand, measurements in a PRE experiment can be focused on one single region of the protein, that is, on a single or few long-range contacts, by using labels. This focused view cannot be obtained in a SAXS experiment. The absence of a statistically significant long-range interaction in our contact map at 293 K is therefore not in contrast to what has been found in the cited NMR study: it only reflects the lower resolution of the SAXS technique with respect to the NMR technique. Conversely, we do find at high temperature the above-mentioned contact; this means that the increase in its statistical occurrence is so high as to be detected also by a low resolution technique. The occurrence of this long-ranging contact was also confirmed by our molecular dynamics simulation, performed at two temperatures encompassing almost the whole experimental range. The contact maps produced by our simulation show indeed that at T = 333 K, after the molecule has collapsed, there is a significant signature of the contact discussed here.

CONCLUSION

In this paper, we have presented a SAXS study of the behavior of tau protein under increasing temperature, pointing out the occurrence of a strong, continuous, thermally induced compaction. The continuous character of the compaction process is demonstrated by the behavior of the Kratky plot and of the fractal dimension d_f, showing a continuous transition from an extended state to a more compact state under increasing temperature from 293 to 333 K. This phenomenon induces a reduction of the protein gyration radius, which decreases monotonously from 7.0 ± 0.2 to 5.6 ± 0.3 nm. Our conformational analysis of SAXS data, performed by means of the EOM package, shows that the collapse of tau is related to an increased propensity to populate compact conformational states under heating, rather than extended conformers. In particular, a high temperature seems to favor the occurrence of a far reaching contact between the region encompassing the end of the P2 domain and the beginning of the repeats domain on one side, and the N-terminal region entailing residues 80−150 on the other. The thermal collapse of the tau protein has been also studied performing the first temperature-dependent computer simulation in explicit water solvent. Our MD simulation confirms the identification of the tau regions involved in the compaction process, as provided by SAXS. The results discussed above show how the binding domain is statistically less affected by the temperature variations as compared to the highly flexible projection domain, which has a key role in the stabilization and organization of microtubules due to its entropic bristle role. This approach seems to be a powerful tool to draw structural information on the interaction between projection domain and repeats domain; this interaction could influence both the entropic bristle role and the MT surface stabilizing function of protein tau. More in general, the approach here described could be useful for a better understanding of intrinsically disordered proteins.

ASSOCIATED CONTENT

Supporting Information

Protein purity has been asseyed by SDS-PAGE. An amount of 5 μg of soluble hTau40 protein, purchased from Sigma (product code: T0-576) obtained from the same stock used for the SAXS experiment and subjected to the same thermal treatment, was resolved on 12% SDS-PAGE. MW: SeeBlue Plus2 Pre-Stained Standard, Invitrogen (cat. no. LC5925) (Figure S1). As shown in Figure S1, protein purity is >90% at 20 °C, and the molecular mass is consistent with about 46 kD, which is the expected value for the tau isoform with 441 residues. At higher temperatures (40 and 60 °C), tau protein does not exhibit significant modifications, pointing out that the thermal treatment does not induce protein aggregation. This material is available free of charge via the Internet at http://pubs.acs.org.

AUTHOR INFORMATION

Notes

The authors declare no competing financial interest.

ACKNOWLEDGMENTS

The computer simulation was supported by CASPUR (Italy) under a Standard HPC Grant 2011 to one of the authors (A.T.).

REFERENCES

(1) Tompa, P. *Structure and Function of Intrinsically Disorderd Proteins*; Taylor Francis Group: Boca Raton, FL, 2010.

(2) Nettels, D; Mueller-Spaeth, S.; Kuester, F.; Hofmann, H; Haenni, D.; Rueegger, S; Reymond, L; Hofmann, A; Kubelka, J; Heinz, B; Gast, K; Best, R.-B.; Schuler, B. Single-molecule spectroscopy of the temperature-induced collapse of unfolded proteins. *Proc. Natl. Acad. Sci. U.S.A.* **2009**, *106*, 20740−20745.

(3) Uversky, V. Intrinsically Disordered Proteins and Their Environment: Effects of Strong Denaturants, Temperature, pH, Counter Ions, Membranes, Binding Partners, Osmolytes, and Macromolecular Crowding. *Protein J.* **2009**, *28*, 305−325.

(4) Shkumatov, A.-V.; Chinnathambi, S.; Mandelkow, E.; Svergun, D.-I. Structural memory of natively unfolded tau protein detected by small-angle X-ray scattering. *Proteins: Struct., Funct., Bioinf.* **2011**, *79*, 2122−2131.

(5) Sadqi, M.; Lapidus, L.-J.; Muoz, V. How fast is protein hydrophobic collapse. *Proc. Natl. Acad. Sci. U.S.A.* **2003**, *100*, 12117−12122.

(6) Noppert, A.; Gast, K.; Marlies, M.-F.; Zirwer, D.; Damaschun, G. Reduced-denatured ribonuclease A is not in a compact state. *FEBS Lett.* **1996**, *380*, 179−182.

(7) Gast, K.; Zirwer, D.; Damaschun, H.; Hahn, U.; Marlies, M.-F.; Wirth, M.; Damaschun, G. Ribonuclease T1 has different dimensions in the thermally and chemically denatured states: a dynamic light scattering study. *FEBS Lett.* **1997**, *403*, 245−248.

(8) Tompa, P. Intrinsically unstructured protein. *Trends Biochem. Sci.* **2002**, *27*, 527−533.
(9) Goedert, M.; Spillantini, M.-G.; Potier, M.-C.; Ulrich, J.; Crowther, R.-A. Cloning and sequencing of the cDNA encoding an isoform of microtubule-associated protein tau containing four tandem repeats: differential expression of tau protein mRNAs in human brain. *EMBO J.* **1989**, *8*, 393−399.
(10) Rosenberg, K.-J.; Kenneth, J.; Ross, J.-L.; Feinstein, H.-E.; Feinstein, S.-C.; Israelachvili, J. Complementary dimerization of microtubule-associated tau protein: Implications for microtubule bundling and tau-mediated pathogenesis. *Proc. Natl. Acad. Sci. U.S.A.* **2008**, *105*, 7445−7450.
(11) Avila, J.; Lucas, J.-J.; Prez, M.; Hernández, F. Role of Tau Protein in Both Physiological and Pathological Conditions. *Physiol. Rev.* **2004**, *84*, 361−384.
(12) von Bergen, M.; Barghorn, S.; Biernat, J.; Mandelkow, E.-M.; Mandelkow, E. Tau aggregation is driven by a transition from random coil to beta sheet structure. *Biochim. Biophys. Acta, Mol. Basis Dis.* **2005**, *1739*, 158−166.
(13) von Bergen, M.; Friedhoff, P.; Biernat, J.; Heberle, J.; Mandelkow, E.-M.; Mandelkow, E. Assembly of tau protein into Alzheimer paired helical filaments depends on a local sequence motif (^{306}VQIVYK^{311}) forming β structure. *Proc. Natl. Acad. Sci. U.S.A.* **2000**, *97*, 5129−5134.
(14) Mukrasch, M.-D.; Bibow, S.; Korukottu, J.; Jeganathan, J.; Sadasivam, J.; Biernat, J.; Griesinger, C.; Mandelkow, E.; Zweckstetter, M. Structural Polymorphism of 441-Residue Tau at Single Residue Resolution. *PLoS Biol.* **2009**, *7* (e1000034), 0399−0414.
(15) Spires-Jones, T.-L; Stoothoff, W.-H.; de Calignon, A.; Jones, P.-B.; Hyman, B.-T. Tau pathophysiology in neurodegeneration: a tangled issue. *Trends Neurosci.* **2009**, *32*, 150−159.
(16) Svergun, D.; Koch, M. Small-angle scattering studies of biological macromolecules in solution. *Rep. Prog. Phys.* **2003**, *66*, 1735−1782.
(17) Ciasca, G.; Papi, M.; Chiarpotto, M.; Rodio, M.; Campi, G.; Rossi, C.; De Sole, P.; Bianconi, A. Transient state kinetic investigation of ferritin iron release. *Appl. Phys. Lett.* **2012**, *100* (073703), 1−3.
(18) De Spirito, M; Arcovito, G.; Papi, M.; Rocco, M.; Ferri, F. Small- and wide-angle elastic light scattering study of fibrin structure. *J. Appl. Crystallogr.* **2003**, *36*, 636−641.
(19) Caracciolo, G.; Pozzi, D.; Caminiti, R.; Amenitsch, H. Lipid mixing upon deoxyribonucleic acid-induced liposomes fusion investigated by small-angle x-ray scattering. *Appl. Phys. Lett.* **2005**, *87*, 133901.
(20) Campi, G.; Ricci, A.; Guagliardi, A.; Giannini, C.; Lagomarsino, S.; Cancedda, R.; Mastrogiacomo, M.; Cedola, A. Early stage mineralization in tissue engineering mapped by high resolution X-ray microdiffraction. *Acta Biomater.* **2012**, *8*, 3411−3418.
(21) Mylonas, E.; Hascher, A.; Bernadó, P.; Blackledge, M.; Mandelkow, E.; Svergun, D.-I. Domain Conformation of Tau Protein Studied by Solution Small-Angle X-ray Scattering. *Biochemistry* **2008**, *47*, 10345−10353.
(22) Schweers, O.; Schnbrunn-Hanebeck, E.; Marx, A.; Mandelkow, E. Structural studies of tau protein and Alzheimer paired helical filaments show no evidence for beta-structure. *J. Biol. Chem.* **1994**, *269*, 24290−24297.
(23) Bernadó, P.; Mylonas, E.; Petoukhov, M.-V.; Blackledge, M.; Svergun, D.-I. Structural Characterization of Flexible Proteins Using Small-Angle X-ray Scattering. *J. Am. Chem. Soc.* **2007**, *129*, 5656−5664.
(24) Laemmli, U.-K. Cleavage of Structural Proteins during the Assembly of the Head of Bacteriophage T4. *Nature* **1970**, *227*, 680−685.
(25) Pernot, P.; Theveneau, P.; Giraud, T.; Nogueira, R.-F.; Nurizzo, D.; Spruce, D.; Surr, J.; McSweeney, S.; Round, A.; Felisaz, F.; Foedinger, L.; Gobbo, A.; Huet, J.; Villard, C.; Cipriani, F. New beamline dedicated to solution scattering from biological macromolecules at the ESRF. *J. Phys.: Conf. Ser.* **2010**, *247*, 012009.
(26) EOM manual, http://www.embl-hamburg.de/biosaxs/eom.html.
(27) GROMACS, release 4.5.3, www.gromacs.org; box volume = 15253 nm^3; G53a6 force field; time step 2 fs; modified Berendsen thermostat, Parrinello-Rahman pressure coupling.
(28) Battisti, A.; Tenenbaum, A. Molecular Dynamics simulation of intrinsically disordered proteins. *Mol. Simul.* **2012**, *38*, 139−143.
(29) Battisti, A.; Ciasca, G.; Grottesi, A.; Bianconi, A.; Tenenbaum, A. Temporary secondary structures in tau, an intrinsically disordered protein. *Mol. Simul.* **2012**, *38*, 525−533.
(30) Kohn, J.-E.; et al. Random-coil behavior and the dimensions of chemically unfolded proteins. *Proc. Natl. Acad. Sci. U.S.A.* **2004**, *101*, 12491−12496.
(31) Papi, M.; Arcovito, G.; De Spirito, M; Amiconi, G.; Bellelli, A.; Boumis, G. Simultaneous static and dynamic light scattering approach to the characterization of the different fibrin gel structures occurring by changing chloride concentration. *Appl. Phys. Lett.* **2005**, *86* (183901), 1−3.
(32) De Spirito, M.; Brunelli, R.; Mei, G.; Bertani, F.-R.; Ciasca, G.; Greco, G.; Papi, M.; Arcovito, G.; Ursini, F.; Parasassi, T. Low Density Lipoprotein Aged in Plasma Forms Clusters Resembling Subendothelial Droplets: Aggregation via Surface Sites. *Biophys. J.* **2006**, *90*, 4239−4247.